

NOAA Atlas NESDIS 51

WORLD OCEAN ATLAS 2001 VOLUME 3: Oxygen

Ricardo A. Locarnini
Todd D. O'Brien
Hernan E. Garcia
John I. Antonov
Timothy P. Boyer
Margarita E. Conkright
Cathy Stephens

Editor: Sydney Levitus

National Oceanographic Data Center
Ocean Climate Laboratory

Silver Spring, MD
May 2002

U.S. DEPARTMENT OF COMMERCE
Donald L. Evans, Secretary

National Oceanic and Atmospheric Administration
Vice Admiral Conrad C. Lautenbacher, Jr. USN (Ret.)
Under Secretary of Commerce for Oceans and Atmosphere

National Environmental Satellite, Data, and Information Service
Gregory W. Withee, Assistant Administrator

National Oceanographic Data Center

Additional copies of this publication, as well as information about NODC data holdings, and services, are available on request directly from NODC. NODC information and data are also available over the Internet through the NODC World Wide site.

National Oceanographic Data Center
User Services Team
NOAA/NESDIS E/OC1
SSM3, 4th Floor
1315 East-West Highway
Silver Spring, MD 20910-3282

Telephone: (301)713-3277

Fax: (301)713-3302

E-mail: services@nodc.noaa.gov

NODC World Wide Web site: <http://www.nodc.noaa.gov/OC5>

For updates on the data, documentation and additional information about WOA01 please refer to:

<http://www.nodc.noaa.gov>

click on: Ocean Climate Laboratory

click on: Products

This publication should be cited as:

R.A. Locarnini, T.D. O'Brien, H.E. Garcia, J.I. Antonov, T.P. Boyer, M.E. Conkright, C. Stephens, 2002: *World Ocean Atlas 2001, Volume 3: Oxygen*. S. Levitus, Ed., NOAA Atlas NESDIS 51, U.S. Government Printing Office, Wash., D.C., 286 pp.

Contents

Preface	xii
Acknowledgments	xiii
Abstract	1
1. Introduction	1
2. Data and data distribution	1
2.1 Data sources	2
2.2 Data quality control	2
2.2a Duplicate elimination	2
2.2b Range checks and gradient checks	2
2.2c Statistical checks	3
2.2d Subjective flagging of data	3
2.2e Representativeness of the data	3
2.2f Calculation of derived quantities	4
3. Data processing procedures	4
3.1 Vertical interpolation to standard levels	4
3.2 Methods of analysis	4
3.2a Overview	4
3.2b Derivation of Barnes (1964) weight function	5
3.2c Derivation of Barnes (1964) response function	6
3.2d Choice of response function	7
3.2e First-guess field determination	7
3.3 Choice of objective analysis procedures	8
3.4 Choice of spatial grid	8
4. Results	8
4.1 Computation of annual and seasonal fields	8
4.2 Explanation of standard level figures	8
4.3 Standard level analyses	9
4.4 Contents of the <i>World Ocean Atlas 2001</i> CD-ROM	9
5. Summary	9
6. Future work	10
7. References	11
8. Appendix A: Annual distribution by one-degree squares of the number of oxygen observations and the mean at selected standard levels for the climatological annual compositing period	23
9. Appendix B: Seasonal distribution of oxygen observations, seasonal mean, and seasonal minus annual means at selected standard levels	47
10. Appendix C: Monthly distribution of oxygen observations, monthly mean, and monthly minus annual means at selected standard levels	87

11. Appendix D:	Annual distribution by one-degree squares of the number of apparent oxygen utilization and percent oxygen saturation observations, and the apparent oxygen utilization mean at selected standard levels for the climatological annual compositing period	147
12. Appendix E:	Seasonal distribution by one-degree squares of the number of apparent oxygen utilization and percent oxygen saturation observations, and the apparent oxygen utilization seasonal mean at selected standard levels	171
13. Appendix F:	Monthly distribution by one-degree squares of the number of apparent oxygen utilization and percent oxygen saturation observations, and the apparent oxygen utilization monthly mean at selected standard levels	195
14. Appendix G:	Annual percent oxygen saturation mean at selected standard levels for the climatological annual compositing period	231
15. Appendix H:	Seasonal percent oxygen saturation mean at selected standard levels	247
16. Appendix I:	Monthly percent oxygen saturation mean at selected standard levels	263

List of Tables

Table 1	Acceptable distances (m) for defining interior and exterior values used in the Reiniger-Ross scheme for interpolating observed level data to standard levels.
Table 2	Response function of the objective analysis scheme as a function of wavelength for WOA01 and earlier analyses.
Table 3	Basins defined for objective analysis and the shallowest depth level for which each basin is defined.

List of Figures

Fig. 1a.	Annual oxygen standard deviation (ml/l) at 500 meters depth by one-degree squares.
Fig. 1b.	Annual oxygen standard error of the mean (ml/l) at 500 meters depth by one-degree squares.
Fig. 2.	Response function of the WOA01, WOA98, WOA94, and Levitus (1982) objective analysis schemes.
Fig. 3.	Scheme used in computing annual, seasonal, and monthly objectively analyzed means for a variable.
Fig. 4.	Annual observed one-degree square oxygen mean value minus objectively analyzed annual mean oxygen values (ml/l) at 500 meters depth.

APPENDIX A

Fig. A1.	Annual oxygen observations at the surface.
Fig. A2.	Annual oxygen observations at 50 m depth.
Fig. A3.	Annual oxygen observations at 75 m depth.
Fig. A4.	Annual oxygen observations at 100 m depth.
Fig. A5.	Annual oxygen observations at 150 m depth.
Fig. A6.	Annual oxygen observations at 200 m depth.
Fig. A7.	Annual oxygen observations at 250 m depth.
Fig. A8.	Annual oxygen observations at 400 m depth.
Fig. A9.	Annual oxygen observations at 500 m depth.
Fig. A10.	Annual oxygen observations at 700 m depth.
Fig. A11.	Annual oxygen observations at 1000 m depth.

- Fig. A12. Annual oxygen observations at 1500 m depth.
 Fig. A13. Annual oxygen observations at 2000 m depth.
 Fig. A14. Annual oxygen observations at 2500 m depth.
 Fig. A15. Annual oxygen observations at 3000 m depth.
 Fig. A16. Annual oxygen observations at 4000 m depth.
- Fig. A17. Annual mean oxygen (ml/l) at the surface.
 Fig. A18. Annual mean oxygen (ml/l) at 50 m depth.
 Fig. A19. Annual mean oxygen (ml/l) at 75 m depth.
 Fig. A20. Annual mean oxygen (ml/l) at 100 m depth.
 Fig. A21. Annual mean oxygen (ml/l) at 150 m depth.
 Fig. A22. Annual mean oxygen (ml/l) at 200 m depth.
 Fig. A23. Annual mean oxygen (ml/l) at 250 m depth.
 Fig. A24. Annual mean oxygen (ml/l) at 400 m depth.
 Fig. A25. Annual mean oxygen (ml/l) at 500 m depth.
 Fig. A26. Annual mean oxygen (ml/l) at 700 m depth.
 Fig. A27. Annual mean oxygen (ml/l) at 1000 m depth.
 Fig. A28. Annual mean oxygen (ml/l) at 1500 m depth.
 Fig. A29. Annual mean oxygen (ml/l) at 2000 m depth.
 Fig. A30. Annual mean oxygen (ml/l) at 2500 m depth.
 Fig. A31. Annual mean oxygen (ml/l) at 3000 m depth.
 Fig. A32. Annual mean oxygen (ml/l) at 4000 m depth.

APPENDIX B

- Fig. B1. Winter (Jan.-Mar.) oxygen observations at the surface.
 Fig. B2. Winter (Jan.-Mar.) oxygen observations at 75 m depth.
 Fig. B3. Winter (Jan.-Mar.) oxygen observations at 150 m depth.
 Fig. B4. Winter (Jan.-Mar.) oxygen observations at 250 m depth.
 Fig. B5. Spring (Apr.-Jun.) oxygen observations at the surface.
 Fig. B6. Spring (Apr.-Jun.) oxygen observations at 75 m surface.
 Fig. B7. Spring (Apr.-Jun.) oxygen observations at 150 m surface.
 Fig. B8. Spring (Apr.-Jun.) oxygen observations at 250 m surface.
 Fig. B9. Summer (Jul.-Sep.) oxygen observations at the surface.
 Fig. B10. Summer (Jul.-Sep.) oxygen observations at 75 m surface.
 Fig. B11. Summer (Jul.-Sep.) oxygen observations at 150 m surface.
 Fig. B12. Summer (Jul.-Sep.) oxygen observations at 250 m surface.
 Fig. B13. Fall (Oct.-Dec.) oxygen observations at the surface.
 Fig. B14. Fall (Oct.-Dec.) oxygen observations at 75 m surface.
 Fig. B15. Fall (Oct.-Dec.) oxygen observations at 150 m surface.
 Fig. B16. Fall (Oct.-Dec.) oxygen observations at 250 m surface.
- Fig. B17. Winter (Jan.-Mar.) mean oxygen (ml/l) at the surface.
 Fig. B18. Winter (Jan.-Mar.) minus annual oxygen (ml/l) at the surface.
 Fig. B19. Winter (Jan.-Mar.) mean oxygen (ml/l) at 75 m depth.
 Fig. B20. Winter (Jan.-Mar.) minus annual oxygen (ml/l) at 75 m depth.
 Fig. B21. Winter (Jan.-Mar.) mean oxygen (ml/l) at 150 m depth.
 Fig. B22. Winter (Jan.-Mar.) minus annual oxygen (ml/l) at 150 m depth.
 Fig. B23. Winter (Jan.-Mar.) mean oxygen (ml/l) at 250 m depth.
 Fig. B24. Winter (Jan.-Mar.) minus annual oxygen (ml/l) at 250 m depth.
 Fig. B25. Spring (Apr.-Jun.) mean oxygen (ml/l) at the surface.
 Fig. B26. Spring (Apr.-Jun.) minus annual oxygen (ml/l) at the surface.
 Fig. B27. Spring (Apr.-Jun.) mean oxygen (ml/l) at 75 m depth.
 Fig. B28. Spring (Apr.-Jun.) minus annual oxygen (ml/l) at 75 m depth.

- Fig. B29. Spring (Apr.-Jun.) mean oxygen (ml/l) at 150 m depth.
- Fig. B30. Spring (Apr.-Jun.) minus annual oxygen (ml/l) at 150 m depth.
- Fig. B31. Spring (Apr.-Jun.) mean oxygen (ml/l) at 250 m depth.
- Fig. B32. Spring (Apr.-Jun.) minus annual oxygen (ml/l) at 250 m depth.
- Fig. B33. Summer (Jul.-Sep.) mean oxygen (ml/l) at the surface.
- Fig. B34. Summer (Jul.-Sep.) minus annual oxygen (ml/l) at the surface.
- Fig. B35. Summer (Jul.-Sep.) mean oxygen (ml/l) at 75 m depth.
- Fig. B36. Summer (Jul.-Sep.) minus annual oxygen (ml/l) at 75 m depth.
- Fig. B37. Summer (Jul.-Sep.) mean oxygen (ml/l) at 150 m depth.
- Fig. B38. Summer (Jul.-Sep.) minus annual oxygen (ml/l) at 150 m depth.
- Fig. B39. Summer (Jul.-Sep.) mean oxygen (ml/l) at 250 m depth.
- Fig. B40. Summer (Jul.-Sep.) minus annual oxygen (ml/l) at 250 m depth.
- Fig. B41. Fall (Oct.-Dec.) mean oxygen (ml/l) at the surface.
- Fig. B42. Fall (Oct.-Dec.) minus annual oxygen (ml/l) at the surface.
- Fig. B43. Fall (Oct.-Dec.) mean oxygen (ml/l) at 75 m depth.
- Fig. B44. Fall (Oct.-Dec.) minus annual oxygen (ml/l) at 75 m depth.
- Fig. B45. Fall (Oct.-Dec.) mean oxygen (ml/l) at 150 m depth.
- Fig. B46. Fall (Oct.-Dec.) minus annual oxygen (ml/l) at 150 m depth.
- Fig. B47. Fall (Oct.-Dec.) mean oxygen (ml/l) at 250 m depth.
- Fig. B48. Fall (Oct.-Dec.) minus annual oxygen (ml/l) at 250 m depth.

APPENDIX C

- Fig. C1. January oxygen observations at the surface.
- Fig. C2. January oxygen observations at 75 m depth.
- Fig. C3. February oxygen observations at the surface.
- Fig. C4. February oxygen observations at 75 m depth.
- Fig. C5. March oxygen observations at the surface.
- Fig. C6. March oxygen observations at 75 m depth.
- Fig. C7. April oxygen observations at the surface.
- Fig. C8. April oxygen observations at 75 m depth.
- Fig. C9. May oxygen observations at the surface.
- Fig. C10. May oxygen observations at 75 m depth.
- Fig. C11. June oxygen observations at the surface.
- Fig. C12. June oxygen observations at 75 m depth.
- Fig. C13. July oxygen observations at the surface.
- Fig. C14. July oxygen observations at 75 m depth.
- Fig. C15. August oxygen observations at the surface.
- Fig. C16. August oxygen observations at 75 m depth.
- Fig. C17. September oxygen observations at the surface.
- Fig. C18. September oxygen observations at 75 m depth.
- Fig. C19. October oxygen observations at the surface.
- Fig. C20. October oxygen observations at 75 m depth.
- Fig. C21. November oxygen observations at the surface.
- Fig. C22. November oxygen observations at 75 m depth.
- Fig. C23. December oxygen observations at the surface.
- Fig. C24. December oxygen observations at 75 m depth.

- Fig. C25. January mean oxygen (ml/l) at the surface.
- Fig. C26. January minus annual oxygen (ml/l) at the surface.
- Fig. C27. January mean oxygen (ml/l) at 75 m depth.
- Fig. C28. January minus annual oxygen (ml/l) at 75 m depth.
- Fig. C29. February mean oxygen (ml/l) at the surface.
- Fig. C30. February minus annual oxygen (ml/l) at the surface.

- Fig. C31. February mean oxygen (ml/l) at 75 m depth.
- Fig. C32. February minus annual oxygen (ml/l) at 75 m depth.
- Fig. C33. March mean oxygen (ml/l) at the surface.
- Fig. C34. March minus annual oxygen (ml/l) at the surface.
- Fig. C35. March mean oxygen (ml/l) at 75 m depth.
- Fig. C36. March minus annual oxygen (ml/l) at 75 m depth.
- Fig. C37. April mean oxygen (ml/l) at the surface.
- Fig. C38. April minus annual oxygen (ml/l) at the surface.
- Fig. C39. April mean oxygen (ml/l) at 75 m depth.
- Fig. C40. April minus annual oxygen (ml/l) at 75 m depth.
- Fig. C41. May mean oxygen (ml/l) at the surface.
- Fig. C42. May minus annual oxygen (ml/l) at the surface.
- Fig. C43. May mean oxygen (ml/l) at 75 m depth.
- Fig. C44. May minus annual oxygen (ml/l) at 75 m depth.
- Fig. C45. June mean oxygen (ml/l) at the surface.
- Fig. C46. June minus annual oxygen (ml/l) at the surface.
- Fig. C47. June mean oxygen (ml/l) at 75 m depth.
- Fig. C48. June minus annual oxygen (ml/l) at 75 m depth.
- Fig. C49. July mean oxygen (ml/l) at the surface.
- Fig. C50. July minus annual oxygen (ml/l) at the surface.
- Fig. C51. July mean oxygen (ml/l) at 75 m depth.
- Fig. C52. July minus annual oxygen (ml/l) at 75 m depth.
- Fig. C53. August mean oxygen (ml/l) at the surface.
- Fig. C54. August minus annual oxygen (ml/l) at the surface.
- Fig. C55. August mean oxygen (ml/l) at 75 m depth.
- Fig. C56. August minus annual oxygen (ml/l) at 75 m depth.
- Fig. C57. September mean oxygen (ml/l) at the surface.
- Fig. C58. September minus annual oxygen (ml/l) at the surface.
- Fig. C59. September mean oxygen (ml/l) at 75 m depth.
- Fig. C60. September minus annual oxygen (ml/l) at 75 m depth.
- Fig. C61. October mean oxygen (ml/l) at the surface.
- Fig. C62. October minus annual oxygen (ml/l) at the surface.
- Fig. C63. October mean oxygen (ml/l) at 75 m depth.
- Fig. C64. October minus annual oxygen (ml/l) at 75 m depth.
- Fig. C65. November mean oxygen (ml/l) at the surface.
- Fig. C66. November minus annual oxygen (ml/l) at the surface.
- Fig. C67. November mean oxygen (ml/l) at 75 m depth.
- Fig. C68. November minus annual oxygen (ml/l) at 75 m depth.
- Fig. C69. December mean oxygen (ml/l) at the surface.
- Fig. C70. December minus annual oxygen (ml/l) at the surface.
- Fig. C71. December mean oxygen (ml/l) at 75 m depth.
- Fig. C72. December minus annual oxygen (ml/l) at 75 m depth.

APPENDIX D

- Fig. D1. Annual AOU and percent oxygen saturation observations at the surface.
- Fig. D2. Annual AOU and percent oxygen saturation observations at 50 m depth.
- Fig. D3. Annual AOU and percent oxygen saturation observations at 75 m depth.
- Fig. D4. Annual AOU and percent oxygen saturation observations at 100 m depth.
- Fig. D5. Annual AOU and percent oxygen saturation observations at 150 m depth.
- Fig. D6. Annual AOU and percent oxygen saturation observations at 200 m depth.
- Fig. D7. Annual AOU and percent oxygen saturation observations at 250 m depth.
- Fig. D8. Annual AOU and percent oxygen saturation observations at 400 m depth.
- Fig. D9. Annual AOU and percent oxygen saturation observations at 500 m depth.

- Fig. D10. Annual AOU and percent oxygen saturation observations at 700 m depth.
 Fig. D11. Annual AOU and percent oxygen saturation observations at 1000 m depth.
 Fig. D12. Annual AOU and percent oxygen saturation observations at 1500 m depth.
 Fig. D13. Annual AOU and percent oxygen saturation observations at 2000 m depth.
 Fig. D14. Annual AOU and percent oxygen saturation observations at 2500 m depth.
 Fig. D15. Annual AOU and percent oxygen saturation observations at 3000 m depth.
 Fig. D16. Annual AOU and percent oxygen saturation observations at 4000 m depth.
- Fig. D17. Annual mean apparent oxygen utilization (ml/l) at the surface.
 Fig. D18. Annual mean apparent oxygen utilization (ml/l) at 50 m depth.
 Fig. D19. Annual mean apparent oxygen utilization (ml/l) at 75 m depth.
 Fig. D20. Annual mean apparent oxygen utilization (ml/l) at 100 m depth.
 Fig. D21. Annual mean apparent oxygen utilization (ml/l) at 150 m depth.
 Fig. D22. Annual mean apparent oxygen utilization (ml/l) at 200 m depth.
 Fig. D23. Annual mean apparent oxygen utilization (ml/l) at 250 m depth.
 Fig. D24. Annual mean apparent oxygen utilization (ml/l) at 400 m depth.
 Fig. D25. Annual mean apparent oxygen utilization (ml/l) at 500 m depth.
 Fig. D26. Annual mean apparent oxygen utilization (ml/l) at 700 m depth.
 Fig. D27. Annual mean apparent oxygen utilization (ml/l) at 1000 m depth.
 Fig. D28. Annual mean apparent oxygen utilization (ml/l) at 1500 m depth.
 Fig. D29. Annual mean apparent oxygen utilization (ml/l) at 2000 m depth.
 Fig. D30. Annual mean apparent oxygen utilization (ml/l) at 2500 m depth.
 Fig. D31. Annual mean apparent oxygen utilization (ml/l) at 3000 m depth.
 Fig. D32. Annual mean apparent oxygen utilization (ml/l) at 4000 m depth.

APPENDIX E

- Fig. E1. Winter (Jan.-Mar.) AOU and percent oxygen saturation observations at the surface.
 Fig. E2. Winter (Jan.-Mar.) AOU and percent oxygen saturation observations at 75 m depth.
 Fig. E3. Winter (Jan.-Mar.) AOU and percent oxygen saturation observations at 150 m depth.
 Fig. E4. Winter (Jan.-Mar.) AOU and percent oxygen saturation observations at 250 m depth.
 Fig. E5. Spring (Apr.-Jun.) AOU and percent oxygen saturation observations at the surface.
 Fig. E6. Spring (Apr.-Jun.) AOU and percent oxygen saturation observations at 75 m surface.
 Fig. E7. Spring (Apr.-Jun.) AOU and percent oxygen saturation observations at 150 m surface.
 Fig. E8. Spring (Apr.-Jun.) AOU and percent oxygen saturation observations at 250 m surface.
 Fig. E9. Summer (Jul.-Sep.) AOU and percent oxygen saturation observations at the surface.
 Fig. E10. Summer (Jul.-Sep.) AOU and percent oxygen saturation observations at 75 m surface.
 Fig. E11. Summer (Jul.-Sep.) AOU and percent oxygen saturation observations at 150 m surface.
 Fig. E12. Summer (Jul.-Sep.) AOU and percent oxygen saturation observations at 250 m surface.
 Fig. E13. Fall (Oct.-Dec.) AOU and percent oxygen saturation observations at the surface.
 Fig. E14. Fall (Oct.-Dec.) AOU and percent oxygen saturation observations at 75 m surface.
 Fig. E15. Fall (Oct.-Dec.) AOU and percent oxygen saturation observations at 150 m surface.
 Fig. E16. Fall (Oct.-Dec.) AOU and percent oxygen saturation observations at 250 m surface.
- Fig. E17. Winter (Jan.-Mar.) mean apparent oxygen utilization (ml/l) at the surface.
 Fig. E18. Winter (Jan.-Mar.) mean apparent oxygen utilization (ml/l) at 75 m depth.
 Fig. E19. Winter (Jan.-Mar.) mean apparent oxygen utilization (ml/l) at 150 m depth.
 Fig. E20. Winter (Jan.-Mar.) mean apparent oxygen utilization (ml/l) at 250 m depth.
 Fig. E21. Spring (Apr.-Jun.) mean apparent oxygen utilization (ml/l) at the surface.
 Fig. E22. Spring (Apr.-Jun.) mean apparent oxygen utilization (ml/l) at 75 m depth.
 Fig. E23. Spring (Apr.-Jun.) mean apparent oxygen utilization (ml/l) at 150 m depth.
 Fig. E24. Spring (Apr.-Jun.) mean apparent oxygen utilization (ml/l) at 250 m depth.
 Fig. E25. Summer (Jul.-Sep.) mean apparent oxygen utilization (ml/l) at the surface.
 Fig. E26. Summer (Jul.-Sep.) mean apparent oxygen utilization (ml/l) at 75 m depth.

- Fig. E27. Summer (Jul.-Sep.) mean apparent oxygen utilization (ml/l) at 150 m depth.
- Fig. E28. Summer (Jul.-Sep.) mean apparent oxygen utilization (ml/l) at 250 m depth.
- Fig. E29. Fall (Oct.-Dec.) mean apparent oxygen utilization (ml/l) at the surface.
- Fig. E30. Fall (Oct.-Dec.) mean apparent oxygen utilization (ml/l) at 75 m depth.
- Fig. E31. Fall (Oct.-Dec.) mean apparent oxygen utilization (ml/l) at 150 m depth.
- Fig. E32. Fall (Oct.-Dec.) mean apparent oxygen utilization (ml/l) at 250 m depth.

APPENDIX F

- Fig. F1. January AOU and percent oxygen saturation observations at the surface.
- Fig. F2. January AOU and percent oxygen saturation observations at 75 m depth.
- Fig. F3. February AOU and percent oxygen saturation observations at the surface.
- Fig. F4. February AOU and percent oxygen saturation observations at 75 m depth.
- Fig. F5. March AOU and percent oxygen saturation observations at the surface.
- Fig. F6. March AOU and percent oxygen saturation observations at 75 m depth.
- Fig. F7. April AOU and percent oxygen saturation observations at the surface.
- Fig. F8. April AOU and percent oxygen saturation observations at 75 m depth.
- Fig. F9. May AOU and percent oxygen saturation observations at the surface.
- Fig. F10. May AOU and percent oxygen saturation observations at 75 m depth.
- Fig. F11. June AOU and percent oxygen saturation observations at the surface.
- Fig. F12. June AOU and percent oxygen saturation observations at 75 m depth.
- Fig. F13. July AOU and percent oxygen saturation observations at the surface.
- Fig. F14. July AOU and percent oxygen saturation observations at 75 m depth.
- Fig. F15. August AOU and percent oxygen saturation observations at the surface.
- Fig. F16. August AOU and percent oxygen saturation observations at 75 m depth.
- Fig. F17. September AOU and percent oxygen saturation observations at the surface.
- Fig. F18. September AOU and percent oxygen saturation observations at 75 m depth.
- Fig. F19. October AOU and percent oxygen saturation observations at the surface.
- Fig. F20. October AOU and percent oxygen saturation observations at 75 m depth.
- Fig. F21. November AOU and percent oxygen saturation observations at the surface.
- Fig. F22. November AOU and percent oxygen saturation observations at 75 m depth.
- Fig. F23. December AOU and percent oxygen saturation observations at the surface.
- Fig. F24. December AOU and percent oxygen saturation observations at 75 m depth.

- Fig. F25. January mean apparent oxygen utilization (ml/l) at the surface.
- Fig. F26. January mean apparent oxygen utilization (ml/l) at 75 m depth.
- Fig. F27. February mean apparent oxygen utilization (ml/l) at the surface.
- Fig. F28. February mean apparent oxygen utilization (ml/l) at 75 m depth.
- Fig. F29. March mean apparent oxygen utilization (ml/l) at the surface.
- Fig. F30. March mean apparent oxygen utilization (ml/l) at 75 m depth.
- Fig. F31. April mean apparent oxygen utilization (ml/l) at the surface.
- Fig. F32. April mean apparent oxygen utilization (ml/l) at 75 m depth.
- Fig. F33. May mean apparent oxygen utilization (ml/l) at the surface.
- Fig. F34. May mean apparent oxygen utilization (ml/l) at 75 m depth.
- Fig. F35. June mean apparent oxygen utilization (ml/l) at the surface.
- Fig. F36. June mean apparent oxygen utilization (ml/l) at 75 m depth.
- Fig. F37. July mean apparent oxygen utilization (ml/l) at the surface.
- Fig. F38. July mean apparent oxygen utilization (ml/l) at 75 m depth.
- Fig. F39. August mean apparent oxygen utilization (ml/l) at the surface.
- Fig. F40. August mean apparent oxygen utilization (ml/l) at 75 m depth.
- Fig. F41. September mean apparent oxygen utilization (ml/l) at the surface.
- Fig. F42. September mean apparent oxygen utilization (ml/l) at 75 m depth.
- Fig. F43. October mean apparent oxygen utilization (ml/l) at the surface.
- Fig. F44. October mean apparent oxygen utilization (ml/l) at 75 m depth.

- Fig. F45. November mean apparent oxygen utilization (ml/l) at the surface.
- Fig. F46. November mean apparent oxygen utilization (ml/l) at 75 m depth.
- Fig. F47. December mean apparent oxygen utilization (ml/l) at the surface.
- Fig. F48. December mean apparent oxygen utilization (ml/l) at 75 m depth.

APPENDIX G

- Fig. G1. Annual mean percent oxygen saturation at the surface.
- Fig. G2. Annual mean percent oxygen saturation at 50 m depth.
- Fig. G3. Annual mean percent oxygen saturation at 75 m depth.
- Fig. G4. Annual mean percent oxygen saturation at 100 m depth.
- Fig. G5. Annual mean percent oxygen saturation at 150 m depth.
- Fig. G6. Annual mean percent oxygen saturation at 200 m depth.
- Fig. G7. Annual mean percent oxygen saturation at 250 m depth.
- Fig. G8. Annual mean percent oxygen saturation at 400 m depth.
- Fig. G9. Annual mean percent oxygen saturation at 500 m depth.
- Fig. G10. Annual mean percent oxygen saturation at 700 m depth.
- Fig. G11. Annual mean percent oxygen saturation at 1000 m depth.
- Fig. G12. Annual mean percent oxygen saturation at 1500 m depth.
- Fig. G13. Annual mean percent oxygen saturation at 2000 m depth.
- Fig. G14. Annual mean percent oxygen saturation at 2500 m depth.
- Fig. G15. Annual mean percent oxygen saturation at 3000 m depth.
- Fig. G16. Annual mean percent oxygen saturation at 4000 m depth.

APPENDIX H

- Fig. H1. Winter (Jan.-Mar.) mean percent oxygen saturation at the surface.
- Fig. H2. Winter (Jan.-Mar.) mean percent oxygen saturation at 75 m depth.
- Fig. H3. Winter (Jan.-Mar.) mean percent oxygen saturation at 150 m depth.
- Fig. H4. Winter (Jan.-Mar.) mean percent oxygen saturation at 250 m depth.
- Fig. H5. Spring (Apr.-Jun.) mean percent oxygen saturation at the surface.
- Fig. H6. Spring (Apr.-Jun.) mean percent oxygen saturation at 75 m surface.
- Fig. H7. Spring (Apr.-Jun.) mean percent oxygen saturation at 150 m surface.
- Fig. H8. Spring (Apr.-Jun.) mean percent oxygen saturation at 250 m surface.
- Fig. H9. Summer (Jul.-Sep.) mean percent oxygen saturation at the surface.
- Fig. H10. Summer (Jul.-Sep.) mean percent oxygen saturation at 75 m surface.
- Fig. H11. Summer (Jul.-Sep.) mean percent oxygen saturation at 150 m surface.
- Fig. H12. Summer (Jul.-Sep.) mean percent oxygen saturation at 250 m surface.
- Fig. H13. Fall (Oct.-Dec.) mean percent oxygen saturation at the surface.
- Fig. H14. Fall (Oct.-Dec.) mean percent oxygen saturation at 75 m surface.
- Fig. H15. Fall (Oct.-Dec.) mean percent oxygen saturation at 150 m surface.
- Fig. H16. Fall (Oct.-Dec.) mean percent oxygen saturation at 250 m surface.

APPENDIX I

- Fig. I1. January mean percent oxygen saturation at the surface.
- Fig. I2. January mean percent oxygen saturation at 75 m depth.
- Fig. I3. February mean percent oxygen saturation at the surface.
- Fig. I4. February mean percent oxygen saturation at 75 m depth.
- Fig. I5. March mean percent oxygen saturation at the surface.

- Fig. I6. March mean percent oxygen saturation at 75 m depth.
- Fig. I7. April mean percent oxygen saturation at the surface.
- Fig. I8. April mean percent oxygen saturation at 75 m depth.
- Fig. I9. May mean percent oxygen saturation at the surface.
- Fig. I10. May mean percent oxygen saturation at 75 m depth.
- Fig. I11. June mean percent oxygen saturation at the surface.
- Fig. I12. June mean percent oxygen saturation at 75 m depth.
- Fig. I13. July mean percent oxygen saturation at the surface.
- Fig. I14. July mean percent oxygen saturation at 75 m depth.
- Fig. I15. August mean percent oxygen saturation at the surface.
- Fig. I16. August mean percent oxygen saturation at 75 m depth.
- Fig. I17. September mean percent oxygen saturation at the surface.
- Fig. I18. September mean percent oxygen saturation at 75 m depth.
- Fig. I19. October mean percent oxygen saturation at the surface.
- Fig. I20. October mean percent oxygen saturation at 75 m depth.
- Fig. I21. November mean percent oxygen saturation at the surface.
- Fig. I22. November mean percent oxygen saturation at 75 m depth.
- Fig. I23. December mean percent oxygen saturation at the surface.
- Fig. I24. December mean percent oxygen saturation at 75 m depth.

Preface

The oceanographic analyses described by this atlas series expand on earlier works, *e.g.* the *World Ocean Atlas 1998* (WOA98), *World Ocean Atlas 1994* (WOA94) and *Climatological Atlas of the World Ocean*. Previously published oceanographic objective analyses have proven to be of great utility to the oceanographic, climate research, and operational environmental forecasting communities. Such analyses are used as boundary and/or initial conditions in numerical ocean circulation models and atmosphere-ocean models, for verification of numerical simulations of the ocean, as a form of "sea truth" for satellite measurements such as altimetric observations of sea surface height, for computation of nutrient fluxes by Ekman transport, and for planning oceanographic expeditions.

We have expanded our earlier analyses to include an all-data annual analysis of chlorophyll, monthly analyses of oxygen, and seasonal and monthly analyses of nutrients. Additional data for these variables have become available and there is a need for such analyses of these data in order to:

- 1) study the role of biogeochemical cycles in determining how the earth's climate system works, particularly the vulnerability of ocean ecosystems to climate change (IPCC, 1996);
- 2) help verify remotely sensed estimates of chlorophyll (SeaWiFS, ADEOS missions) which requires knowledge of *in situ* variables such as chlorophyll and plankton;
- 3) provide the most comprehensive set of oceanographic databases and products based on these data to the international research and forecasting communities.

We continue preparing climatological analyses on a one-degree grid. This is because higher resolution analyses are not justified for all the variables we are working with and we wish to produce a set of analyses for which all variables have been analyzed in the same manner. High-resolution analyses as typified by the work of Boyer and Levitus (1997) will be published as separate atlases.

In the acknowledgment section of this publication we have expressed our view that creation of global ocean profile and plankton databases and analyses are only possible through the cooperation of scientists, data managers, and scientific administrators throughout the international scientific community. I would also like to thank my colleagues and the staff of the Ocean Climate Laboratory of NODC for their dedication to the project leading to publication of this atlas series. Their integrity and thoroughness have made this database possible. It is my belief that the development and management of national and international oceanographic data archives is best performed by scientists who are actively working with the historical data.

Sydney Levitus
National Oceanographic Data Center
Silver Spring, MD
May 2002

Acknowledgments

This work was made possible by a grant from the NOAA Climate and Global Change Program which enabled the establishment of a research group at the National Oceanographic Data Center. The purpose of this group is to prepare research quality oceanographic databases, as well as to compute objective analyses of, and diagnostic studies based on, these databases.

The data on which this atlas is based are in *World Ocean Database 2001* and are distributed on-line and CD-ROM by NODC/WDC. Many data were acquired as a result of the NODC *Oceanographic Data Archaeology and Rescue* (NODAR) project, the IOC/IODE *Global Oceanographic Data Archaeology and Rescue* (GODAR) project, and the IOC/IODE *World Ocean Database* project (WOD). At NODC/WDC, “data archaeology and rescue” projects are supported with funding from the NOAA Environmental Science Data and Information Management (ESDIM) Program and the NOAA Climate and Global Change Program which has included support from NASA and DOE. Support for some of the regional IOC/GODAR meetings was provided by the MAST program of the European Union. The European Community has also provided support for the MEDAR/MEDATLAS project which has resulted in the inclusion of substantial amounts of ocean profile data from the Mediterranean and Black Seas into *World Ocean Database 2001*.

We would like to acknowledge the scientists, technicians, and programmers who have submitted data to national and regional data centers as well as the managers and staff at the various data centers. Their efforts have made this and similar works possible.

WORLD OCEAN ATLAS 2001

VOLUME 3: Oxygen

*Ricardo A. Locarnini, Todd D. O'Brien, Hernan E. Garcia, John I. Antonov,
Timothy P. Boyer, Margarita E. Conkright, and Cathy Stephens*
National Oceanographic Data Center
Silver Spring, MD

ABSTRACT

This atlas contains maps of the climatological distribution of dissolved oxygen, apparent oxygen utilization, and percent oxygen saturation at selected standard depth levels of the world ocean on a one-degree grid. Maps for all-data climatological annual, seasonal, and monthly compositing periods are presented at standard depth levels. Seasonal and monthly difference fields from the annual mean fields are presented for dissolved oxygen at selected standard depth levels. The fields used to generate these maps were computed by objective analysis of historical data. Data distribution maps are presented for all-data annual, seasonal, and monthly compositing periods at selected standard levels.

1. INTRODUCTION

This atlas is an analysis of all historical oxygen profile data available from the National Oceanographic Data Center (NODC) and World Data Center (WDC) for Oceanography, Silver Spring, Maryland. Many data have been acquired as a result of several data management projects including:

- a) the Intergovernmental Oceanographic Commission (IOC) *Global Oceanographic Data Archaeology and Rescue* (GODAR) project;
- b) the NODC *Oceanographic Data Archaeology and Rescue* (NODAR) project;
- c) the IOC *World Ocean Database* project (WOD).

Data used in this atlas have been analyzed in a consistent, objective manner on a one-degree latitude-longitude grid at standard oceanographic levels between the surface and ocean bottom to a maximum depth of 5500 m. The procedures used are identical to those used in *World Ocean Atlas 1998*, or WOA98 (O'Brien *et al.*, 1998). These procedures are very similar to those used to produce earlier analyses (Levitus, 1982; Levitus and Boyer, 1994). Annual, seasonal, and monthly analyses have been computed for dissolved oxygen (hereinafter referred to as oxygen), Apparent Oxygen Utilization (AOU), and percent oxygen saturation.

Objective analyses shown in this atlas are limited by the nature of the data base (data are non-synoptic and scattered in space) and characteristics of the objective analysis techniques, and the grid used. These limitations and characteristics will be discussed below.

Since the publication of WOA98, substantial amounts of additional historical data have become available. However, even with these additional data, we are still hampered in a number of ways by a lack of data. Because of the lack of data, we are forced to examine the annual cycle by compositing all data regardless of the year of observation. In some areas, quality control is made difficult by the limited number of data. Data may exist in an area for only one season, thus precluding any representative annual analysis. In some areas there may be a reasonable spatial distribution of data points on which to base an analysis, but there may be only a few (perhaps only one) data in each one-degree latitude-longitude square.

2. DATA AND DATA DISTRIBUTION

Data sources and quality control procedures are briefly described below. For further information on the data sources used in *World Ocean Atlas 2001* (WOA01) refer to the *World Ocean Database 2001* (WOD01) series (Conkright *et al.*, 2002a; Locarnini *et al.*, 2002). The quality control procedures we have used in preparing these analyses are described by Conkright *et al.* (2002b).

2.1 Data sources

Historical Ocean Station Data (OSD) oxygen profiles used in this atlas are from the NODC/WDC archives and includes all data gathered as a result of the NODAR, GODAR, and WOD projects.

Appendix A shows the geographic distribution of all historical oxygen observations at selected standard depth levels, Appendix B shows the distribution of observations for individual seasons, and Appendix C shows the distribution of observations for individual months. Appendix D shows the geographic distribution of all historical apparent oxygen utilization and percent oxygen saturation observations at selected standard depth levels, Appendix E shows the distribution of observations for individual seasons, and Appendix F shows the distribution of observations for individual months. In all data distribution maps that appear in the appendices, a small dot indicates a one-degree square containing one to four observations and a large dot indicates a square containing five or more observations.

We define the terms "standard level data" and "observed level data" here so the reader can understand the various data distribution figures, summary figures, and tables we present in this atlas. We refer to the actual measured value of an oceanographic variable *in situ* (Latin for "in place") as an "observation," and to the depth at which such a measurement was made as the "observed level depth." We may refer to such data as "observed level data." Before the development of oceanographic instrumentation that measure at high frequencies in the vertical, oceanographers often attempted to make measurements at selected "standard levels" in the water column. Sverdrup *et al.* (1942) presented the suggestions of the International Association of Physical Oceanography (IAPSO) as to which depths oceanographic measurements should be made or interpolated to for analysis. Different nations or institutions have a slightly different set of standard levels defined. For many purposes, including preparation of this atlas, observed level data are interpolated to standard observation levels, if such data do not occur exactly at a standard observation levels. We have prepared objective analyses at the NODC standard levels as given in Table 1 and added levels at 3500, 4500, and 5500 m. Section 3.1 discusses the vertical interpolation procedures used in our work.

2.2 Data quality control

Quality control of the data is a major task, the difficulty of which is directly related to lack of data (in some areas) upon which to base statistical checks. Consequently certain empirical criteria were applied, and as part of the last processing step, subjective judgment was used. Individual data, and in some cases entire profiles or cruises, have been

flagged because these data produced features that were judged to be non-representative or in error. As part of our work, we have made available WOD01 which contains both observed level profile data as well as standard level profile data with various quality control flags applied. Our knowledge of the variability of the world ocean now includes a greater appreciation and understanding of the ubiquity of eddies, rings, and lenses in some parts of the world ocean as well as interannual and interdecadal variability of water mass properties associated with modal variability of the atmosphere such as the North Atlantic Oscillation and El Niño/Southern Oscillation. Therefore, we have simply flagged data, not eliminated them. Thus, individual investigators can make their own decision regarding the representativeness or correctness of the data. Investigators studying the distribution of features such as eddies will be interested in those data that we may regard as unrepresentative for the preparation of the analyses shown in this atlas.

2.2a Duplicate elimination

Because data are received from many sources, sometimes the same data set is received at NODC/WDC more than once but with slightly different time and/or position and/or data values, and hence are not easily identified as duplicate stations. Therefore, our databases were checked for the presence of exact and "near" exact replicates using eight different criteria. The first checks involve identifying stations with exact position/date/time and data values; the next checks involve offsets in position/date/time. Profiles identified as duplicates in the checks with a large offset were individually verified to ensure they were indeed duplicate profiles.

All but one profile from each set of replicate profiles were eliminated at the first step of our processing.

2.2b Range checks and gradient checks

Range checking (checking whether data is within set minimum and maximum values as a function of depth) was performed on all data as a first error check to flag and eliminate from further use the relatively few data that seemed to be grossly in error. Range checks were prepared for individual regions of the world ocean. Conkright *et al.* (2002b) and Boyer and Levitus (1994) detail the quality control procedures and include tables showing the ranges selected for each basin.

A check as to whether excessive gradients occur in the data were made for each variable in WOD01 both in terms of positive and negative gradients.

2.2c Statistical checks

Statistical checks were performed as follows. All data for each variable (irrespective of season), at each standard level, were averaged by five-degree latitude-longitude squares to produce a record of the number of observations, mean, and standard deviation in each square. Statistics were computed for the annual, seasonal, and monthly compositing periods. Below 50 m depth, if data were more than three standard deviations from the mean, the data were flagged and eliminated from further use in our objective analyses. Above 50 m depth, a five-standard-deviation criterion was used in five-degree squares that contained any land area. In selected five degree squares that are close to land areas, a four standard-deviation check was used. In all other squares a three-standard-deviation criterion was used.

The reason for the weaker criterion in coastal and near-coastal regions is the exceptionally large variability in the coastal five-degree square statistics for some variables. Frequency distributions of some variables in some coastal regions are observed to be skewed or bimodal. Thus to avoid eliminating possibly good data in highly variable environments, the standard deviation criteria were weakened.

The total number of oxygen measurements in each cast, as well as the total number of observations exceeding the criterion, were recorded. If more than two observations in a cast were found to exceed the standard deviation criterion, then the entire cast was flagged. This check was imposed after tests indicated that surface data from particular casts (which upon inspection appeared to be erroneous) were being flagged but deeper data were not. Other situations were found where erroneous data from the deeper portion of a cast were flagged, while near-surface data from the same cast were not flagged because of larger natural variability in surface layers. One reason for this was the decrease of the number of observations with depth and the resulting change in sample statistics. The standard-deviation check was applied twice to the data set for each compositing period. Individual flags were set for each period.

In summary, first the five-degree square statistics were computed, and the elimination procedure described above was used to provide a preliminary data set. Next, new five-degree-square statistics were computed from this preliminary data set and used with the same statistical check to produce a new, "clean" data set. The reason for applying the statistical check twice was to flag (and eliminate from further use), in the first round, any grossly erroneous or non-representative data from the data set that would artificially increase the variances. The second check is then more effective in eliminating smaller, but still erroneous or non-representative, observations. The standard deviation for dissolved oxygen observations at 500 meters depth on a

one-degree latitude-longitude square is shown in Figure 1a; the standard error of the mean for the same depth is shown in Figure 1b.

2.2d Subjective flagging of data

The data were averaged by one-degree squares for input to the objective analysis program. After initial objective analyses were computed, the input set of one-degree means still contained suspicious data contributing to unrealistic distributions, yielding intense bull's-eyes or gradients. Examination of these features indicated that some of them were due to particular oceanographic cruises. In such cases, data from an entire cruise were eliminated from further use by setting a flag on each profile from the cruise. In other cases, individual profiles or measurements were found to cause these features and were eliminated from use.

2.2e Representativeness of the data

Another quality control issue is data representativeness. The general paucity of data forces the compositing of all historical data to produce "climatological" fields. In a given one-degree square, there may be data from a month or season of one particular year, while in the same or a nearby square there may be data from an entirely different year. If there is large interannual variability in a region where scattered sampling in time has occurred, then one can expect the analysis to reflect this. Because the observations are scattered randomly with respect to time, except for a few limited areas, the results cannot, in a strict sense, be considered a true long-term climatological average.

We present smoothed analyses of historical means, based (in certain areas) on relatively few observations. We believe, however, that useful information about the oceans can be gained through our procedures and that the large-scale features are representative of the real ocean. We believe that, if a hypothetical global synoptic set of ocean data (temperature, salinity, or oxygen) existed, and one were to smooth this data to the same degree as we have smoothed the historical means overall, the large-scale features would be similar to our results. Some differences would certainly occur because of interannual-to-decadal-scale variability.

To clarify discussions of the amount of available data, quality control techniques, and representativeness of the data, the reader should examine in detail the maps showing the distribution of data (Appendices A-F) and the *World Ocean Database 2001* atlas series which shows the distribution of oceanographic stations as a function of year and instrument type. These maps are provided to give the reader a quick, simple way of examining the historical data distributions. Basically, the data diminish in number with increasing depth. In the upper ocean, the all-data annual

mean distributions are quite good for defining large-scale features, but for the seasonal periods, the data base is inadequate for some regions. With respect to the deep ocean, in some areas the distribution of observations may be adequate for some diagnostic computations but inadequate for other purposes. If an isolated deep basin or some region of the deep ocean has only one observation, then no horizontal gradient computations are meaningful. However, useful information is provided by the observation in the computation of other quantities (*e.g.*, a volumetric mean over a major ocean basin).

2.2f Calculation of derived quantities

Apparent Oxygen Utilization (AOU) and percent oxygen saturation were calculated for an oxygen observation when temperature and salinity observations were also present in the profile at the same observed depth.

Oxygen solubility, $[O_{2,s}]$, was computed after Garcia and Gordon (1992). Apparent Oxygen Utilization (AOU) was then calculated as the difference between oxygen solubility and the measured oxygen concentration, $[O_{2,m}]$:

$$AOU = [O_{2,s}] - [O_{2,m}] \quad (1)$$

Percent oxygen saturation, O_p , was calculated as the ratio of measured oxygen concentration, $[O_{2,m}]$, to oxygen solubility, $[O_{2,s}]$, multiplied by 100:

$$O_p = \frac{[O_{2,m}]}{[O_{2,s}]} \times 100 \quad (2)$$

Once derived, based on observed level data, AOU and percent oxygen saturation were processed using the same methods as those applied to (dissolved) oxygen. However, if any of the three calculation variables (temperature, salinity, oxygen) were flagged during processing, the derived AOU and oxygen saturation values were automatically flagged and were not used for interpolation to standard levels.

3. DATA PROCESSING PROCEDURES

3.1 Vertical interpolation to standard levels

Vertical interpolation of observed level data to standard levels followed procedures in JPOTS Editorial Panel (1991). These procedures are in part based on the work of Reiniger and Ross (1968). Four observed level values surrounding the standard level values were used, two values

from above the standard level and two values below the standard level. The pair of values furthest from the standard level are termed "exterior" points and the pair of values closest to the standard level are termed "interior" points. Paired parabolas were generated via Lagrangian interpolation. A reference curve was fitted to the four data points and used to define unacceptable interpolations caused by "overshooting" in the interpolation. When there were too few data points above or below the standard level to apply the Reiniger and Ross technique, we used a three-point Lagrangian interpolation. If three points were not available (either two above and one below or vice-versa), we used linear interpolation. In the event that an observation occurred exactly at the depth of a standard level, then a direct substitution was made. Table 1 provides the range of acceptable distances for which observed level data could be used for interpolation to a standard level.

3.2 Methods of analysis

3.2a Overview

An objective analysis scheme of the type described by Barnes (1964) was used to produce the fields shown in this atlas. This scheme had its origins in the work of Cressman (1959). In *World Ocean Atlas 1994*, or WOA94 (Levitus and Boyer, 1994), the Barnes (1973) scheme was used. This required only one "correction" to the first-guess field at each grid point in comparison to the successive correction method of Cressman (1959) and Barnes (1964). This was to minimize computer time used in the processing. Barnes (1994) recommends a return to a multi-pass analysis when computer time is not an issue. Based on our own experience we agree with this assessment. The single pass analysis, used in WOA94, caused an artificial front in the Southeastern Pacific Ocean in a data sparse area (Anne Marie Treguier, personal communication). The analysis scheme used in generating WOA98 and WOA01 analyses uses a three-pass "correction" which eliminates this artificial front.

Inputs to the analysis scheme were one-degree square means of data values at standard levels (for whatever period and variable being analyzed), and a first-guess value for each square. For instance, one-degree square means for our annual analysis were computed using all available data regardless of date of observation. For July, we used all historical July data regardless of year of observation.

Analysis was the same for all standard depth levels. Each one-degree latitude-longitude square value was defined as being representative of its square. The 360x180 gridpoints are located at the intersection of half-degree lines of latitude and longitude. An influence radius was then specified. At those grid points where there was an observed mean value, the difference between the mean and the first-guess field

was computed. Next, a correction to the first-guess value at all gridpoints was computed as a distance-weighted mean of all gridpoint difference values that lie within the area around the gridpoint defined by the influence radius. Mathematically, the correction factor derived by Barnes (1964) is given by the expression

$$C_{i,j} = \frac{\sum_{s=1}^n W_s Q_s}{\sum_{s=1}^n W_s} \quad (3)$$

where

(i,j) = coordinates of a gridpoint in the east-west and north-south directions respectively;

C_{i,j} = the correction factor at gridpoint coordinates (i,j);

n = the number of observations that fall within the area around the point i,j defined by the influence radius;

Q_s = the difference between the observed mean and the first-guess at the Sth point in the influence area;

**W_s = exp (-E r² R⁻²), for r ≤ R;
= 0, for r > R;**

r = distance of the observation from the gridpoint;

R = influence radius;

E = 4.

The derivation of the weight function, W_s, will be presented in the following section. At each gridpoint we computed an analyzed value G_{i,j} as the sum of the first-guess, F_{i,j}, and the correction C_{i,j}. The expression for this is

$$G_{i,j} = F_{i,j} + C_{i,j} \quad (4)$$

If there were no data points within the area defined by the influence radius, then the correction was zero, the first-guess field was left unchanged, and the analyzed value was simply the first-guess value. This correction procedure was applied at all gridpoints to produce an analyzed field. The resulting field was first smoothed with a median filter

(Tukey, 1974; Rabiner *et al.*, 1975) and then smoothed with a five-point smoother of the type described by Shuman (1957). The choice of first-guess fields is important and we discuss our procedures in section 3.2e.

The analysis scheme is based on the work of several researchers analyzing meteorological data. Bergthorsson and Doos (1955) computed corrections to a first-guess field using various techniques: one assumed that the difference between a first-guess value and an analyzed value at a gridpoint was the same as the difference between an observation and a first-guess value at a nearby observing station. All the observed differences in an area surrounding the gridpoint were then averaged and added to the gridpoint first-guess value to produce an analyzed value. Cressman (1959) applied a distance-related weight function to each observation used in the correction in order to give more weight to observations that occur closest to the gridpoint. In addition, Cressman (1959) introduced the method of performing several iterations of the analysis scheme using the analysis produced in each iteration as the first-guess field for the next iteration. He also suggested starting the analysis with a relatively large influence radius and decreasing it with successive iterations so as to analyze smaller scale phenomena with each pass.

Sasaki (1960) introduced a weight function that was specifically related to the density of observations, and Barnes (1964, 1973) extended the work of Sasaki (1960). The weight function of Barnes (1964) has been used here. The objective analysis scheme we used is in common use by the mesoscale meteorological community. Several studies of objective analysis techniques have been made. Achtemeier (1987) examined the "concept of varying influence radii for a successive corrections objective analysis scheme." Seaman (1983) compared the "objective analysis accuracies of statistical interpolation and successive correction schemes." Smith and Leslie (1984) performed an "error determination of a successive correction type objective analysis scheme." Smith *et al.* (1986) made "a comparison of errors in objectively analyzed fields for uniform and non-uniform station distribution."

3.2b Derivation of Barnes (1964) weight function

The principle upon which Barnes (1964) weight function is derived is that "the two-dimensional distribution of an atmospheric variable can be represented by the summation of an infinite number of independent harmonic waves, that is, by a Fourier integral representation". If f(x,y) is the variable, then in polar coordinates (r,θ), a smoothed or filtered function h(x,y) can be defined:

$$h(x,y) = \frac{1}{2\pi} \int_0^{2\pi} \int_0^{\infty} \eta f(x + r\cos\theta, y + r\sin\theta) d(r^2 / 4K) d\theta \quad (5)$$

where r is the radial distance from a gridpoint whose coordinates are (x,y) . The weight function is defined as

$$\eta = \exp(-r^2 / 4K) \quad (6)$$

which resembles the Gaussian distribution. The shape of the weight function is determined by the value of K , which depends on the distribution of data. The determination of K follows. The weight function has the property that

$$\frac{1}{2\pi} \int_0^{2\pi} \int_0^{\infty} \eta d\left(\frac{r^2}{4K}\right) d\theta = 1. \quad (7)$$

This property is desirable because in the continuous case (5) the application of the weight function to the distribution $f(x,y)$ will not change the mean of the distribution. However, in the discrete case (3), we only sum the contributions to within the distance R . This introduces an error in the evaluation of the filtered function, because the condition given by (7) does not apply. The error can be pre-determined and set to a reasonably small value in the following manner. If one carries out the integration in (7) with respect to θ , the remaining integral can be rewritten as

$$\int_0^R \eta d\left(\frac{r^2}{4K}\right) + \int_R^{\infty} \eta d\left(\frac{r^2}{4K}\right) = 1. \quad (8)$$

Defining the second integral as ε yields

$$\int_0^R \exp\left(-\frac{r^2}{4K}\right) d\left(\frac{r^2}{4K}\right) = 1 - \varepsilon \quad (9)$$

from which

$$\varepsilon = \exp(-R^2 / 4K) \quad (10)$$

Levitus (1982) chose $\varepsilon = 0.02$, which implies with respect to (9) the representation of 98 percent of the influence of any data around the gridpoint in the area defined by the influence radius, R . In terms of the weight function used in the evaluation of (3) this choice leads to a value of $E=4$ since

$$E = R^2 / 4K = -\ln \varepsilon. \quad (11)$$

Thus,

$$K = R^2 / 16. \quad (12)$$

The choice of ε and the specification of R determine the shape of the weight function.

Barnes (1964) proposed using this scheme in an iterative fashion similar to Cressman (1959). Levitus (1982) used a four iteration scheme with a variable influence radius for each pass. Levitus and Boyer (1994) used a one-iteration scheme. WOA98 and WOA01 use a three iteration scheme with a variable influence radius. The three influence radii are 888, 666, and 444 km.

3.2c Derivation of Barnes (1964) response function

It is desirable to know the response of a data set to the interpolation procedure applied to it. Following Barnes (1964) we let

$$f(x) = A \sin(ax) \quad (13)$$

in which, $a = 2\pi/\lambda$ with λ being the wavelength of a particular Fourier component, and substitute this function into equation (5) along with the expression for η in equation (6). Then

$$g(x) = D(A \sin(ax)) = Df(x) \quad (14)$$

in which D is the response function for one application of the analysis. The phase of each Fourier component is not changed by the interpolation procedure. The results of an analysis pass are used as the first-guess for the next analysis pass in an iterative fashion. The response function after N iterations as derived by Barnes (1964) is

$$g_n = f(x) D \sum_{n=1}^{N=1} (1 - D)^{n-1} \quad (15)$$

Equation (15) differs trivially from that given by Barnes. The difference is due to our first-guess field being defined as a zonal average, annual mean, seasonal mean, or monthly mean, whereas Barnes used the first application of the analysis as a first-guess. Barnes (1964) also showed

that applying the analysis scheme in an iterative fashion will result in convergence of the analyzed field to the observed data field. However, it is not desirable to approach the observed data too closely, because at least seven or eight gridpoints are needed to represent a Fourier component.

The response function given in (15) is useful in two ways: it is informative to know what Fourier components make up the analyses, and the computer programs used in generating the analyses can be checked for correctness by comparison with (15).

3.2d Choice of response function

The distribution of observations (see Appendices) at different depths and for the different averaging periods, are not regular in space or time. At one extreme, regions exist in which every one-degree square contains data and no interpolation needs to be performed. At the other extreme are regions in which few if any data exist. Thus, with variable data spacing the average separation distance between gridpoints containing data is a function of geographical position and averaging period. However, if we computed and used a different average separation distance for each variable at each depth and each averaging period, we would be generating analyses in which the wavelengths of observed phenomena might differ from one depth level to another and from one season to another. In WOA94, a fixed influence radius of 555 kilometers was used to allow uniformity in the analysis of all variables. For this analyses, a three-pass analysis, based on Barnes (1964), with influence radii of 888, 666 and 444 km was used.

Inspection of (3) shows that the difference between the analyzed field and the first-guess at any gridpoint is proportional to the sum of the weighted-differences between the observed mean and first-guess at all gridpoints containing data within the influence area.

The reason for using the five-point smoother and the median smoother is that our data are not evenly distributed in space. As the analysis moves from regions containing data to regions devoid of data, small-scale discontinuities may develop. The five-point and median smoothers are used to eliminate these discontinuities. The five-point smoother does not affect the phase of the Fourier components that comprise an analyzed field.

The response function for the analyses presented in this atlas is given in Table 2 and Figure 2. For comparison purposes, the response function used by Levitus (1982) and Levitus and Boyer (1994) are also presented. The response function represents the smoothing inherent in the objective analysis described above plus the effects of one application of the five-point smoother and one application of a five-point median smoother. The effect of varying the amount

of smoothing in North Atlantic sea surface temperature (SST) fields has been quantified by Levitus (1982) for a particular case. In a region of strong SST gradient such as the Gulf Stream, the effect of smoothing can easily be responsible for differences between analyses exceeding 1.0°C.

To avoid the problem of the influence region extending across land or sills to adjacent basins, the objective analysis program uses basin "identifiers" to preclude the use of data from adjacent basins. Table 3 lists these basins and the depth at which no exchange of information between basins is allowed during the objective analysis of data, i.e., "depths of mutual exclusion." Some regions are nearly, but not completely, isolated topographically. Because some of these nearly isolated basins have water mass properties that are different from surrounding basins, we have chosen to treat these as isolated basins as well. Not all such basins have been identified because of the complicated structure of the sea floor. In Table 3, a region marked with a "*" can interact with adjacent basins except for special areas such as the Isthmus of Panama.

3.2e First-guess field determination

For all variables and compositing periods, there are gaps in the data coverage. In some parts of the world ocean, there exist adjacent basins whose water mass properties are individually nearly homogeneous but have distinct basin-to-basin differences. Spurious features can be created when an influence area extends over two basins of this nature (basins are listed in Table 3). Our choice of first-guess field attempts to minimize the creation of these features. To provide a first-guess field for the annual analysis at any standard level, we first zonally averaged the observed data in each one-degree latitude belt by individual ocean basins. An annual analysis of a variable was then used as the first-guess for each seasonal analysis and each seasonal analysis was used as a first-guess for the appropriate monthly analysis if computed.

We then reanalyzed the data for each variable using the newly produced analyses as first-guess fields described as follows and as shown in Figure 3. A new annual mean was computed as the mean of the twelve monthly analyses for the upper 1500 m, and the mean of the four seasons below 1500 m depth. This new annual mean was used as the first-guess field for new seasonal analyses. These new seasonal analyses were used to produce new monthly analyses. This procedure produces slightly smoother means. More importantly we recognize that fairly large data-void regions exist, in some cases to such an extent that a seasonal or monthly analysis in these regions is not meaningful. We are interested in computing integral quantities such as heat storage that are deviations from annual means. Geographic distribution of observations for the all-data annual periods

(see appendices) is excellent for upper layers of the ocean. By using an all-data annual mean, first-guess field regions where data exists for only one season or month will show no contribution to the annual cycle. By contrast, if we used a zonal average for each season or month, then, in those latitudes where gaps exist, the first-guess field would be heavily biased by the few data points that exist. If these were anomalous data in some way, an entire basin-wide belt might be affected.

One advantage of producing "global" fields for a particular compositing period (even though some regions are data void) is that such analyses can be modified by investigators for use in modeling studies. For example, England (1992) noted that the temperature distribution produced by Levitus (1982) for the Antarctic is too high (due to a lack of winter data for the Southern Hemisphere) to allow for the formation of Antarctic Intermediate Water in an ocean general circulation model. By decreasing the temperature of the "observed" field the model was able to produce this water mass.

3.3 Choice of objective analysis procedures

Optimum interpolation (Gandin, 1963) has been used by some investigators to objectively analyze oceanographic data. We recognize the power of this technique but have not used it to produce analyzed fields. As described by Gandin (1963), optimum interpolation is used to analyze synoptic data using statistics based on historical data. In particular, second-order statistics such as correlation functions are used to estimate the distribution of first order parameters such as means. We attempt to map most fields in this atlas based on relatively sparse data sets. By necessity we must composite all data regardless of year of observation, to have enough data to produce a global, hemispheric, or regional analysis for a particular month or season. Because of the paucity of data, we prefer not to use an analysis scheme that is based on second order statistics. In addition, as Gandin (1963) has noted, there are two limiting cases associated with optimum interpolation. The first is when a data distribution is dense. In this case, the choice of interpolation scheme makes little difference. The second case is when data are sparse. In this case, an analysis scheme based on second order statistics is of questionable value. For additional information on objective analysis procedures see Thiebaut and Pedder (1987) and Daley (1991).

3.4 Choice of spatial grid

The analyses that comprise WOA98 and WOA01 have been computed using a new land-sea topography to define ocean depths at each grid point (ETOPO5, 1988). From the ETOPO5 mask, a quarter-degree mask was created based on ocean bottom depth and land criteria. If four or more 5-minute square values out of a possible nine in a one-quarter-

degree box were defined as land, then the quarter-degree gridbox was defined to be land. If no more than two of the 5-minute squares had the same depth value in a quarter-degree box, then the average value of the 5-minute ocean depths in that box was defined to be the depth of the quarter-degree gridbox. If three or more 5-minute squares out of the nine had a common bottom depth, then the depth of the quarter-degree box was set to the most common depth value. The same method was used to go from a quarter-degree to a one-degree resolution. In the one-degree resolution case, at least four points out of a possible sixteen (in a one-degree square) had to be land in order for the one-degree square to remain land and three out of sixteen had to have the same depth for the ocean depth to be set. These criteria yielded a mask that was then modified by:

- a) Connecting the Isthmus of Panama,
- b) maintaining an opening in the Straits of Gibraltar and in the English Channel,
- c) connecting the Kamchatka Peninsula and the Baja Peninsula to their respective continents.

The quarter-degree mask was created as an intermediate step to ensure consistency between the present work and future high resolution analysis of temperature and salinity.

4. RESULTS

4.1 Computation of annual and seasonal fields

After completion of all of our analyses we define a final annual analysis as the average of our twelve monthly mean fields in the upper 1500 m of the ocean. Below 1500 m depth we define an annual analysis as the mean of the four seasonal analyses. Our final seasonal analyses are defined as the average of monthly analyses in the upper 1500 m of the ocean - see Figure 3.

4.2 Explanation of standard level figures

All figures showing standard level analyses in this atlas series use similar symbols for displaying information. Continents are indicated as solid - black areas. Ocean areas shallower than the standard depth level being displayed are gray. For apparent oxygen utilization, regions with values less than zero are dot stippled. For percent oxygen saturation, regions with values greater than 100 are dot stippled. Gridpoints for which there were less than four one-degree-square values available to correct the first-guess are indicated by an X. "H" and "L" indicate locations of the absolute maximum and minimum of the entire field. All figures were computer drafted.

4.3 Standard level analyses

Global distributions of annual mean oxygen, apparent oxygen utilization, and percent oxygen saturation at standard analysis levels are presented in Appendices A, D, and G. Seasonal analyses are presented in Appendices B, E, and H. Seasonal mean minus annual mean difference fields, for dissolved oxygen, are also presented in Appendix B. Monthly analyses are presented in Appendices C, F, and I. Monthly mean minus annual mean difference fields, for dissolved oxygen, are also presented in Appendix C.

4.4 Contents of the *World Ocean Atlas 2001* CD-ROM

This atlas presents data for selected standard levels of the world oceans. Associated with this atlas is a CD-ROM containing two parts: digital fields (for each dissolved oxygen, apparent oxygen utilization, and percent oxygen saturation) for the world ocean, and figures illustrating these data for the World, Pacific, Atlantic, and Indian basins;

- (a) fields containing the number of observations by one-degree squares as a function of depth;
- (b) one-degree annual objectively analyzed fields at 33 standard levels;
- (c) one-degree seasonal objectively analyzed fields at 33 standard levels;
- (d) one-degree seasonal minus annual analyses at 33 standard levels;
- (e) one-degree monthly objective at 24 standard levels;
- (f) one-degree monthly minus annual analyses at 24 standard levels;
- (g) one-degree fields of the annual standard deviation at 33 standard depth levels;
- (h) one-degree fields of the seasonal standard deviation at 33 standard depth levels;
- (i) one-degree fields of the monthly standard deviation at 24 standard depth levels;
- (j) one-degree fields of the annual standard error of the mean at 33 standard depth levels;
- (k) one-degree fields of the seasonal standard error of the mean at 33 standard depth levels;
- (l) one-degree fields of the monthly standard error of the mean at 24 standard depth levels;

- (m) one-degree unanalyzed annual mean minus objectively analyzed mean values at 33 standard depth levels. These fields represent the combined interpolation and smoothing “error” of our analyses. An example of these statistics is shown in Figure 4;
- (n) one-degree unanalyzed seasonal mean minus objectively analyzed seasonal mean values at 33 standard levels;
- (o) one-degree unanalyzed monthly mean minus objectively analyzed monthly mean values for 24 depth levels;
- (p) land-sea file used in the analysis;
- (q) definition of ocean basin masks used in the analysis.

In addition, we present figures of the unanalyzed annual, seasonal, and monthly mean fields (input into the objective analysis) and the number of gridpoints within the influence regions for all standard levels listed above.

The sample standard deviation in a gridbox was computed using:

$$s = \sqrt{\frac{\sum_{n=1}^N (x_n - \bar{x})^2}{N - 1}} \quad (16)$$

in which x_n = the n^{th} data value in the gridbox, \bar{x} = mean of all data values in the gridbox, and N = total number of data values in the gridbox. The standard error of the mean was computed by dividing the standard deviation by the square root of the number of observations in each gridbox.

5. SUMMARY

In the preceding sections we have described the results of a project to objectively analyze all historical oxygen data archived at NODC/WDC, including substantial amounts of data gathered as a result of the NODC and IOC data archaeology and rescue projects. We desire to build a set of climatological analyses that are as similar as possible in all respects for all variables including relatively data sparse variables such as nutrients. This provides investigators with a consistent set of analyses to work with.

One advantage of the analysis techniques used in this atlas is that we know the amount of smoothing by objective analyses as given by the response function in Table 2 and

Figure 2. We believe this to be an important function for constructing and describing a climatology of any geophysical parameter. Particularly when computing anomalies from a standard climatology, it is important that the synoptic field be smoothed to the same extent as the climatology, to prevent generation of spurious anomalies simply through differences in smoothing. A second reason is that purely diagnostic computations require a minimum of seven or eight gridpoints to represent any Fourier component with accuracy. Higher order derivatives will require more smoothing.

We have attempted to create objectively analyzed fields and data sets that can be used as a "black box." We emphasize that some quality control procedures used are subjective. For those users who wish to make their own choices, all the data used in our analyses are available both at standard depth levels as well as observed depth levels (*World Ocean Database 2001* CD-ROM set - Conkright *et al.*, 2002b). The results presented in this atlas show some features that are suspect and may be due to nonrepresentative or incorrect data that were not flagged by the quality control techniques used. Although we have attempted to eliminate as many of these features as possible by flagging the data which generate these features some obviously remain. Some may eventually turn out not to be artifacts but rather to represent real features, not yet capable of being described in a meaningful way due to lack of data.

6. FUTURE WORK

Our analyses will be updated when justified by additional observations. As more data are received at NODC/WDC, we will also be able to produce improved annual and seasonal climatologies for each variable as Boyer and Levitus (1997) have done for temperature and salinity.

References

- Achtemeier, G. L., 1987: On the concept of varying influence radii for a successive corrections objective analysis. *Monthly Weather Review*, 11, 1761-1771.
- Barnes, S. L., 1964: A technique for maximizing details in numerical weather map analysis. *J. App. Meteor.*, 3, 396-409.
- _____, 1973: Mesoscale objective map analysis using weighted time series observations. *NOAA Technical Memorandum ERL NSSL-62*, 60 pp.
- _____, 1994: Applications of the Barnes Objective Analysis Scheme, Part III: Tuning for Minimum Error. *J. Atmosph. and Oceanic Tech.* 11:1459-1479.
- Bergthorsson, P., and B. Doos, 1955: Numerical Weather map analysis. *Tellus*, 7, 329-340.
- Boyer, T. P., and S. Levitus, 1994: Quality control and processing of historical temperature, salinity and oxygen data. *NOAA Technical Report NESDIS 81*, 65 pp.
- Boyer, T.P., and S. Levitus, 1997: *Objective Analyses of temperature and salinity for the world ocean on a 1/4 °grid*. *NOAA/NESDIS Atlas 11*. U.S. Gov. Printing Office, Wash., D.C., 62 pp.
- Conkright, M.E., J.I. Antonov, O. Baranova, T. P. Boyer, H.E. Garcia, R. Gelfeld, D. Johnson, R.A. Locarnini, P.P. Murphy, T.D. O'Brien, I. Smolyar, C. Stephens, 2002a: *World Ocean Database 2001, Volume 1: Introduction*. S. Levitus, Ed., NOAA Atlas NESDIS 42, U.S. Government Printing Office, Washington, D.C., 167 pp., CD-ROMs.
- Conkright, M. E., T. O'Brien, T.P. Boyer, C. Stephens, R. A. Locarnini, H. E. Garcia, P. P. Murphy, D. Johnson, O. Baranova, J. I. Antonov, R. Tatusko, R. Gelfeld, I. Smolyar, 2002b: *World Ocean Database 2001 CD-ROM Data Set Documentation*. National Oceanographic Data Center, Silver Spring, MD, 137 pp.
- Cressman, G. P., 1959: An operational objective analysis scheme. *Mon. Wea. Rev.*, 87, 329-340.
- Daley, R., 1991: *Atmospheric Data Analysis*. Cambridge University Press, Cambridge, 457 pp.
- England, M.H., 1992: On the formation of Antarctic Intermediate and Bottom Water in Ocean general circulation models. *J. Phys. Oceanogr.*, 22, 918- 926.
- ETOPO5, 1988: Data Announcements 88-MGG-02, Digital relief of the Surface of the Earth. NOAA, National Geophysical Data Center, Boulder, CO.
- IPCC (Intergovernmental Panel on Climate Change) 1996: *Climate Change 1995 - The Science of Climate Change, Contribution of Working Group I to the Second Assessment Report of the Intergovernmental Panel on Climate Change*. Editors J.J. Houghton, L.G. Meiro Filho, B.A. Callander, N. Harris, A. Kattenberg, and K. Maskell. Cambridge University Press, Cambridge, UK, 572 pp.
- Gandin, L.S., 1963: *Objective Analysis of Meteorological fields*. Gidrometeorol Izdat, Leningrad (translation by Israel program for Scientific Translations, Jerusalem, 1966); 242 pp.
- Garcia, H.I., and L. I. Gordon, 1992: Oxygen solubility in seawater: Better fitting equations. *Limnol. Oceanogr.*, 37(6), 1307-1312.
- Levitus, S., 1982: *Climatological Atlas of the World Ocean*, NOAA Professional Paper No. 13, U.S. Gov. Printing Office, 173 pp.

- Levitus, S., and T. Boyer, 1994: *World Ocean Atlas 1994, Vol 2: Oxygen*. NOAA Atlas NESDIS 2, Wash., D.C., 186 pp.
- Locarnini, R. A., M.E. Conkright, T.P. Boyer, J. I. Antonov, O. K. Baranova, H. E. Garcia, R. Gelfeld, D. Johnson, P. P. Murphy, T. D. O'Brien, I. Smolyar, C. Stephens, 2002: *World Ocean Database 2001, Volume 4: Temporal Distribution of Temperature, Salinity, and Oxygen Profiles*. S. Levitus, Ed., NOAA Atlas NESDIS 45, U.S. Government Printing Office, Washington, D.C., 332 pp., CD-ROMs
- O'Brien, T., S. Levitus, T. P. Boyer, M.E. Conkright, J. I. Antonov, C. Stephens, 1998: *World Ocean Atlas 1998, Volume 7: Oxygen of the Atlantic Ocean*. NOAA Atlas NESDIS 33, U.S. Government Printing Office, Washington., D.C., 234 pp, CD-ROMs.
- Rabiner, L. R., M. R. Sambur, and C. E. Schmidt, 1975: *Applications of a nonlinear smoothing algorithm to speech processing*, *IEEE Trans. on Acoustics, Speech and Signal Processing*, Vol. Assp-23, 552-557.
- Reiniger, R.F., and C.F. Ross, 1968: A method of interpolation with application to oceanographic data. *Deep-Sea Res.*, 9, 185-193.
- Sasaki, Y., 1960: An objective analysis for determining initial conditions for the primitive equations. Ref. 60-1 6T, Atmospheric Research Lab., Univ. of Oklahoma Research Institute, Norman, 23 pp.
- Seaman, R. S., 1983: Objective Analysis accuracies of statistical interpolation and successive correction schemes. *Australian Meteor. Mag.*, 31, 225-240.
- Shuman, F. G., 1957: Numerical methods in weather prediction: II. Smoothing and filtering. *Mon. Wea. Rev.*, 85, 357-361.
- Smith, D. R., and F. Leslie, 1984: Error determination of a successive correction type objective analysis scheme. *J. Atm. and Oceanic Tech.*, 1, 121-130.
- Smith, D.R., M.E. Pumphry, and J.T. Snow, 1986: A comparison of errors in objectively analyzed fields for uniform and nonuniform station distribution, *J. Atm. Oceanic Tech.*, 3, 84-97.
- Sverdrup, H.U., M.W. Johnson, and R.H. Fleming, 1942: *The Oceans: Their physics, chemistry, and general biology*. Prentice Hall, 1060 pp.
- Thiebaux, H.J., M.A. Pedder, 1987: *Spatial Objective Analysis: with applications in atmospheric science*. Academic Press, 299 pp.
- Tukey, J. W., 1974: Nonlinear (nonsuperposable) methods for smoothing data, in "*Cong. Rec.*", 1974 EASCON, 673 pp.
- JPOTS (Joint Panel on Oceanographic Tables and Standards) Editorial Panel, 1991: *Processing of Oceanographic Station Data*. UNESCO, Paris, 138 pp.

Table 1. Acceptable distances (m) for defining interior and exterior values used in the Reiniger-Ross scheme for interpolating observed level data to standard levels.

Standard Level number	Standard depths (m)	Acceptable distances (m) for interior values	Acceptable distances (m) for exterior values
1	0	5	200
2	10	50	200
3	20	50	200
4	30	50	200
5	50	50	200
6	75	50	200
7	100	50	200
8	125	50	200
9	150	50	200
10	200	50	200
11	250	100	200
12	300	100	200
13	400	100	200
14	500	100	400
15	600	100	400
16	700	100	400
17	800	100	400
18	900	200	400
19	1000	200	400
20	1100	200	400
21	1200	200	400
22	1300	200	1000
23	1400	200	1000
24	1500	200	1000
25	1750	200	1000
26	2000	1000	1000
27	2500	1000	1000
28	3000	1000	1000
29	3500	1000	1000
30	4000	1000	1000
31	4500	1000	1000
32	5000	1000	1000
33	5500	1000	1000

Table 2. Response function of the objective analysis scheme as a function of wavelength for WOA01 and earlier analyses.

Wavelength*	Levitus (1982)	WOA94	WOA98 - WOA01
360ΔX	1.000	0.999	1.000
180ΔX	1.000	0.997	0.999
120ΔX	1.000	0.994	0.999
90ΔX	1.000	0.989	0.998
72ΔX	1.000	0.983	0.997
60ΔX	1.000	0.976	0.995
45ΔX	1.000	0.957	0.992
40ΔX	0.999	0.946	0.990
36ΔX	0.999	0.934	0.987
30ΔX	0.996	0.907	0.981
24ΔX	0.983	0.857	0.969
20ΔX	0.955	0.801	0.952
18ΔX	0.923	0.759	0.937
15ΔX	0.828	0.671	0.898
12ΔX	0.626	0.532	0.813
10ΔX	0.417	0.397	0.698
9ΔX	0.299	0.315	0.611
8ΔX	0.186	0.226	0.500
6ΔX	3.75×10^{-2}	0.059	0.229
5ΔX	1.34×10^{-2}	0.019	0.105
4ΔX	1.32×10^{-3}	2.23×10^{-3}	2.75×10^{-2}
3ΔX	2.51×10^{-3}	1.90×10^{-4}	5.41×10^{-3}
2ΔX	5.61×10^{-7}	5.30×10^{-7}	1.36×10^{-6}

* For ΔX = 111 km

Table 3. Basins defined for objective analysis and the shallowest standard depth level for which each basin is defined.

BASIN	STANDARD DEPTH	BASIN	STANDARD DEPTH
Aleutian Basin	28	Gulf of Mexico	26
Andaman Basin	25	Hudson Bay	1
Arabian Sea	30	Indian Ocean	1 *
Arctic Ocean	1 *	Java Sea	6
Argentine Basin	31	Kara Sea	8
Atlantic Indian Basin	31	Marianas Basin	30
Atlantic Ocean	1 *	Mascarene Basin	30
Baffin Bay	14	Mediterranean Sea	1 *
Baltic Sea	1	North Caribbean	26
Banda Sea	23	North American Basin	29
Barents Sea	28	Pacific Ocean	1 *
Bay of Bengal	1 *	Persian Gulf	1
Beaufort Sea	28	Philippine Sea	30
Black Sea	1	Red Sea	1
Brazil Basin	31	Sea of Okhotsk	19
Caribbean Sea	23	Sea of Japan	1
Caspian Sea	1	Somali Basin	30
Celebes Sea	25	South China Sea	28
Central Indian Basin	29	Southeast Pacific Basin	29
Chile Basin	30	Southeast Indian Basin	29
Coral Sea	29	Southeast Atlantic Basin	29
Crosat Basin	30	Southern Ocean	1 *
East Atlantic Indian Basin	32	Southwest Atlantic Basin	29
East Indian Basin	29	Sulu Sea	10
East Mediterranean	16	Sulu Sea II	14
East Caroline Basin	30	Tasman Sea	30
Fiji Basin	29	Venezuela Basin	14
Guatemala Basin	29	West Mediterranean	19
Guinea Basin	30	West European Basin	29

Basins marked with a “” can interact with adjacent basins

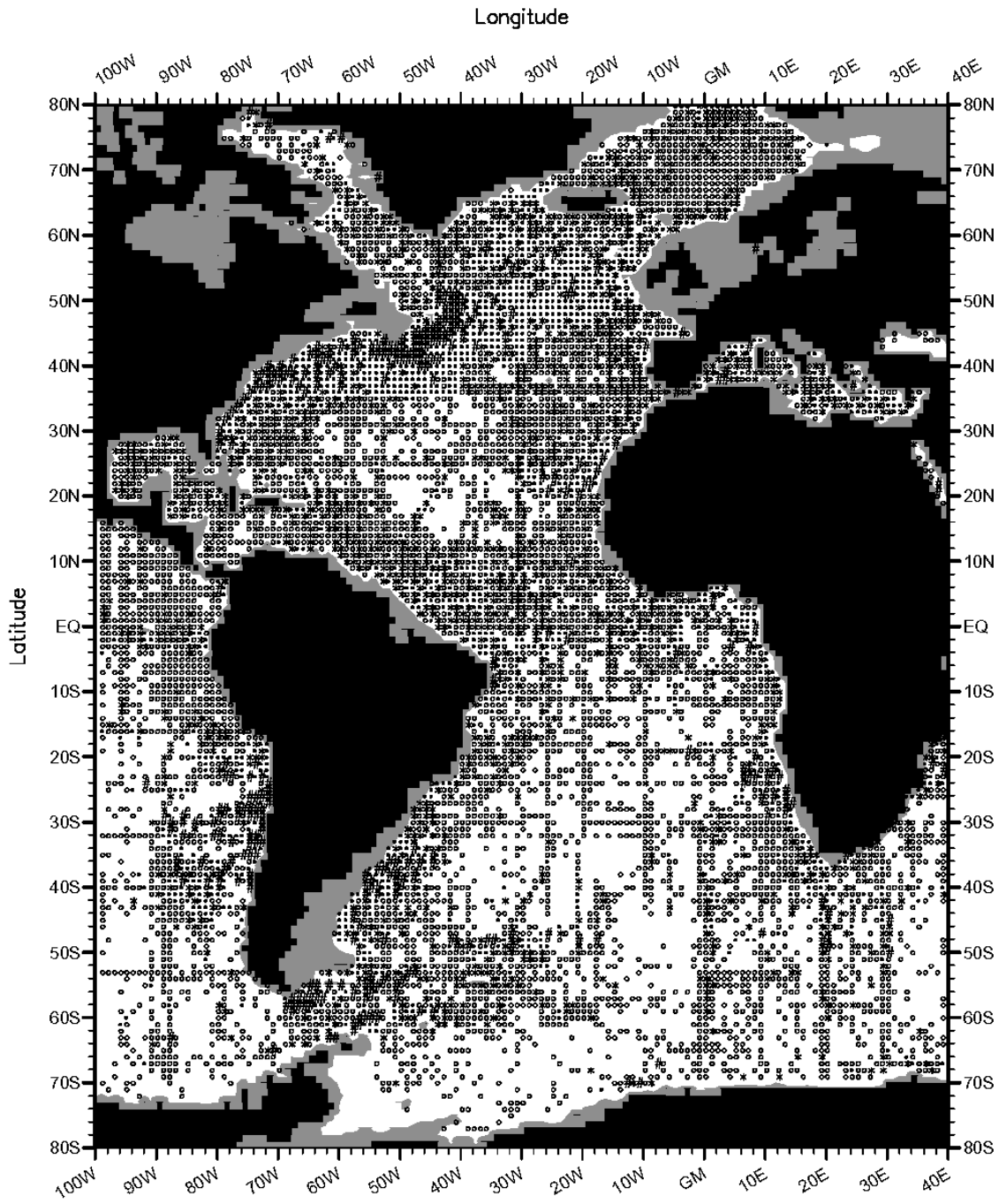


Fig. 1a. Annual oxygen standard deviation (ml/l) at 500 meters depth by one-degree squares.

$\leq 0.15 = \circ$
 0.15 - 0.25 = *
 0.25 - 0.5 = •
 > 0.5 = #

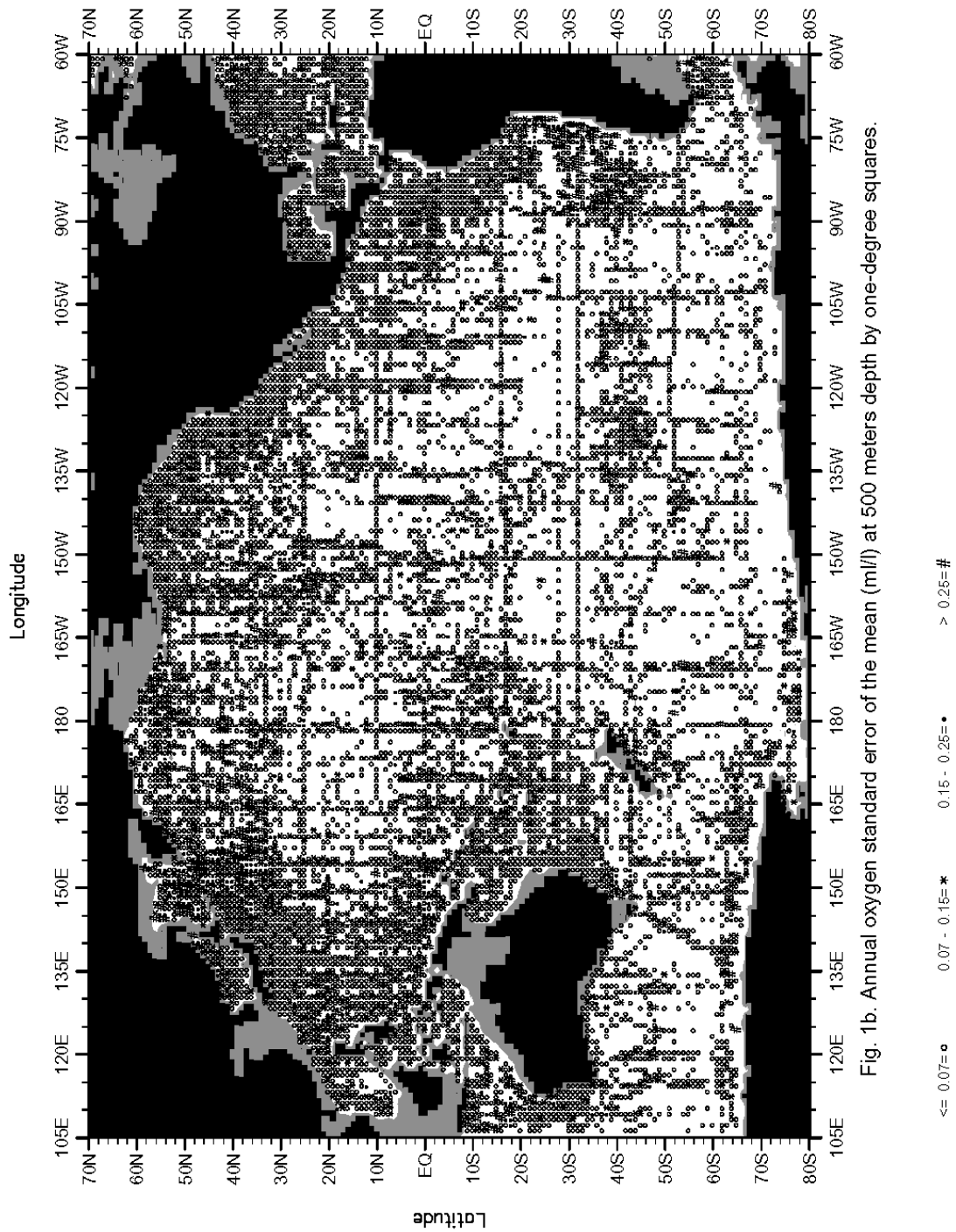


Fig. 1b. Annual oxygen standard error of the mean (m/l) at 500 meters depth by one-degree squares.

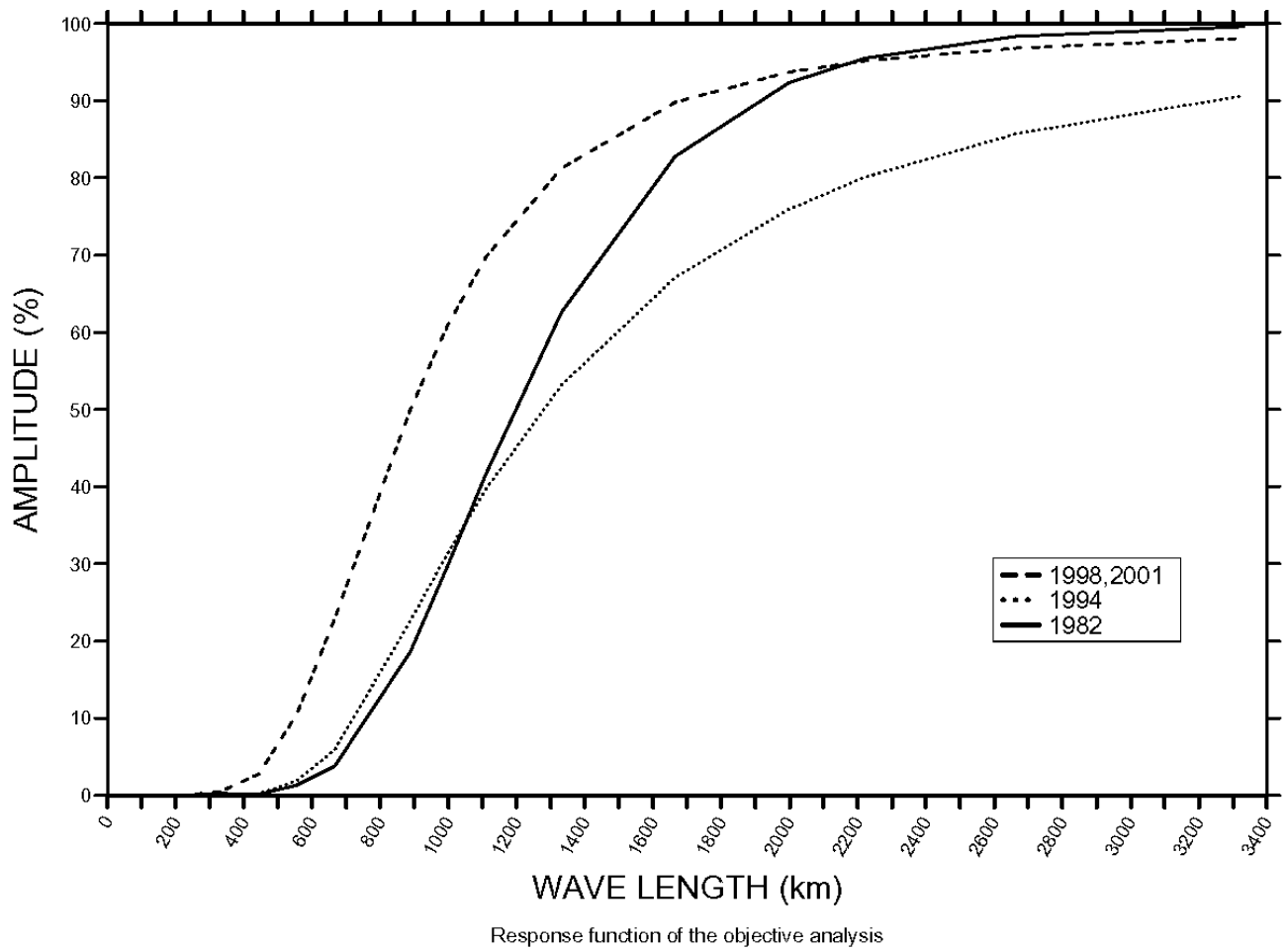


Figure 2. Response function of the WOA01, WOA98, WOA94, and Levitus (1982) objective analysis schemes.

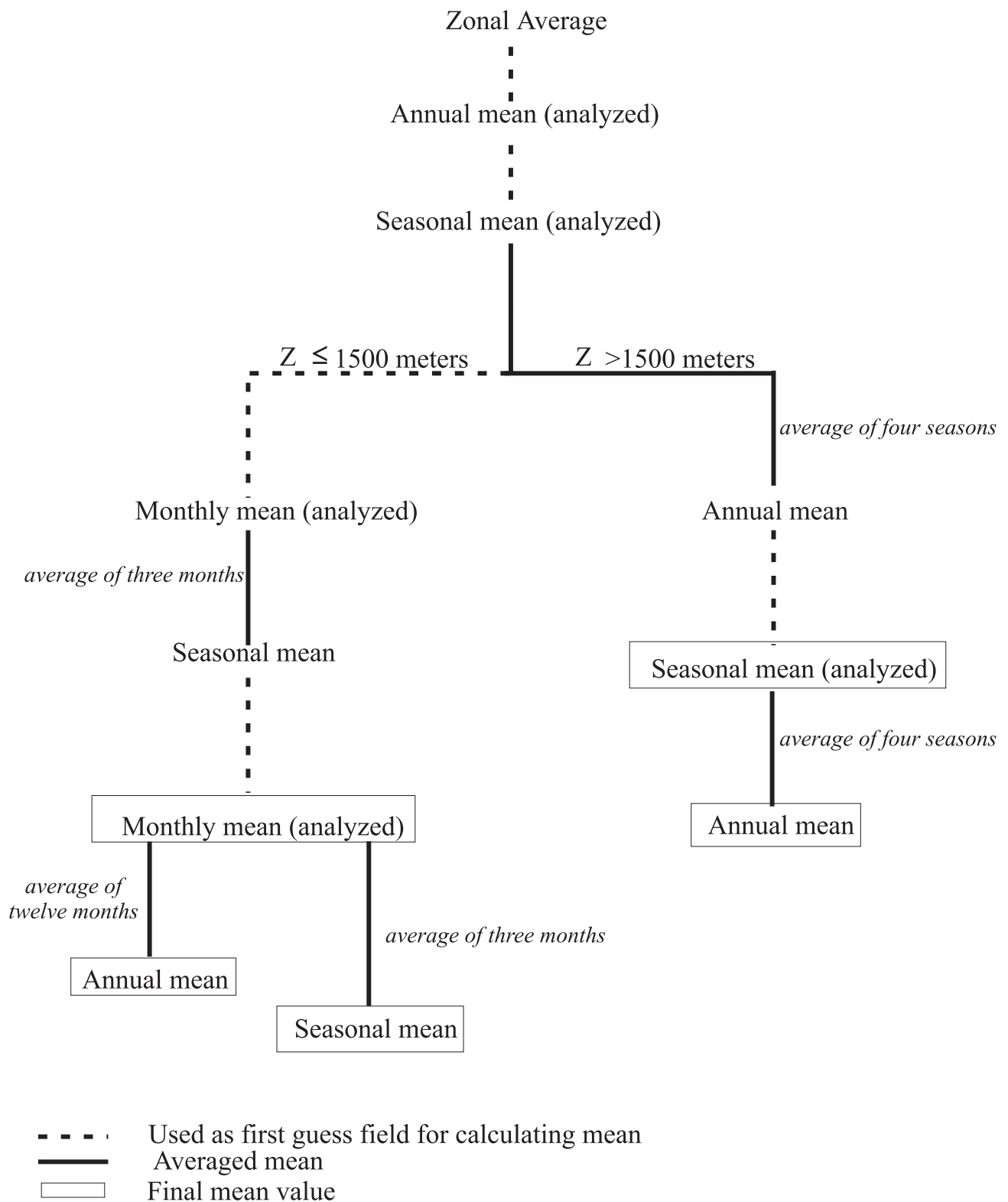


Figure 3. Scheme used in computing annual, seasonal, and monthly objectively analyzed means for a variable.



Fig. 4. Annual observed one-degree square oxygen mean value minus objectively analyzed annual mean oxygen values (m/l) at 500 meters depth.

APPENDICES

In each data distribution figure in each appendix, a small dot indicates a one-degree square containing 1-4 observations and a large dot indicates a one-degree square containing five or more observations.

In each figure showing an objectively analyzed mean field or difference between seasonal (monthly) mean and annual mean, gridpoints for which there were less than four one-degree square values available to correct the first-guess are indicated by an “x”.

